

Figure 1. The ROI with biofilm structure during the image characterization process (time = 0). (a) Raw grayscale image, (b) binary image with a threshold of 0.3, (c) binary image after hole filling and noise removal, (d) binary image after opening operation, following by a second-time hole filling.

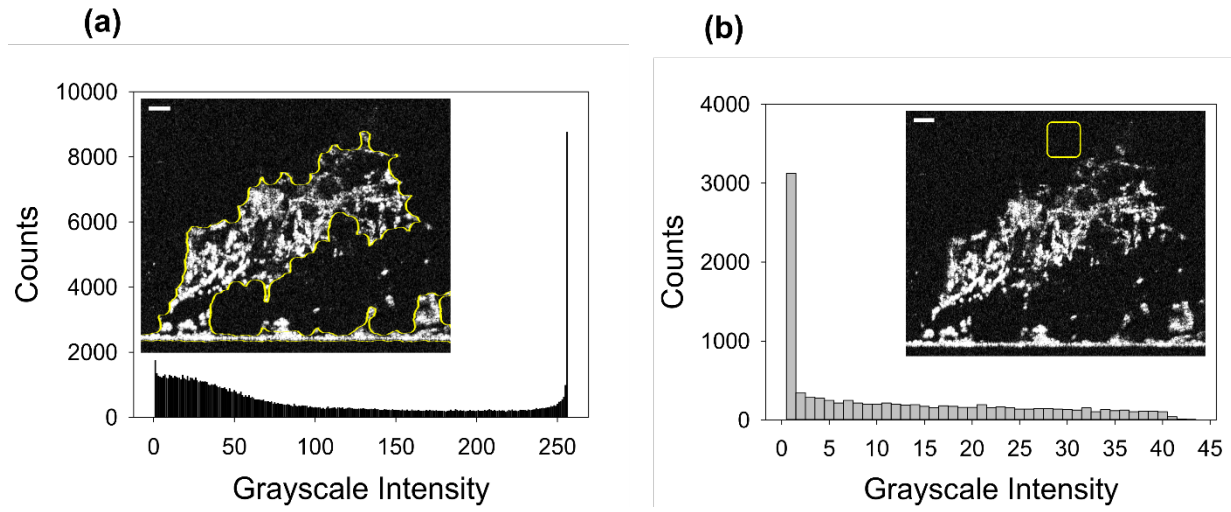


Figure 2. Histograms of grayscale intensity for biofilm structure (a) and background (b). The selected biofilm and background grayscale area is shown as a subplot of (a) and (b), respectively.

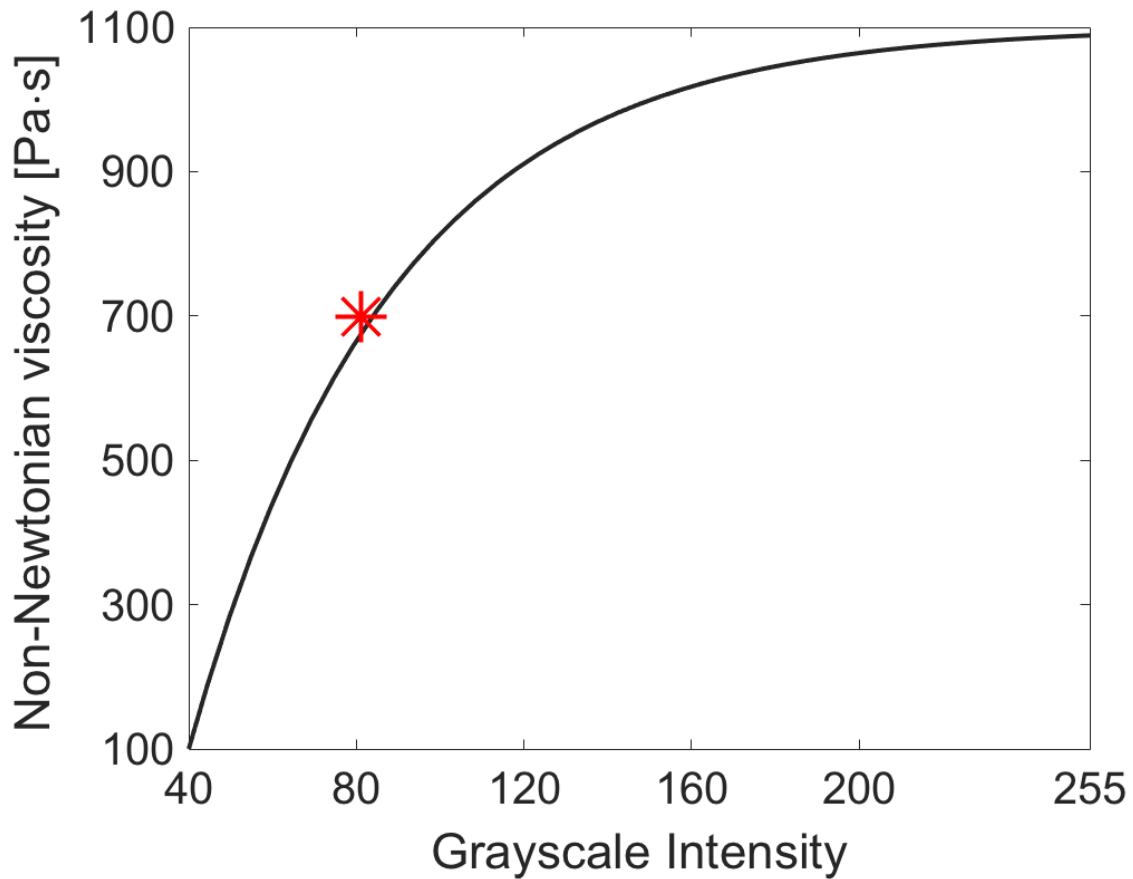


Figure 3. Weibull function representing non-Newtonian viscosity with corresponding grayscale intensities. The red starred marker represents an averaged viscosity value of $\mu_b = 699$ Pa·s measured from the rheometer test and is associated with the average grayscale intensity.

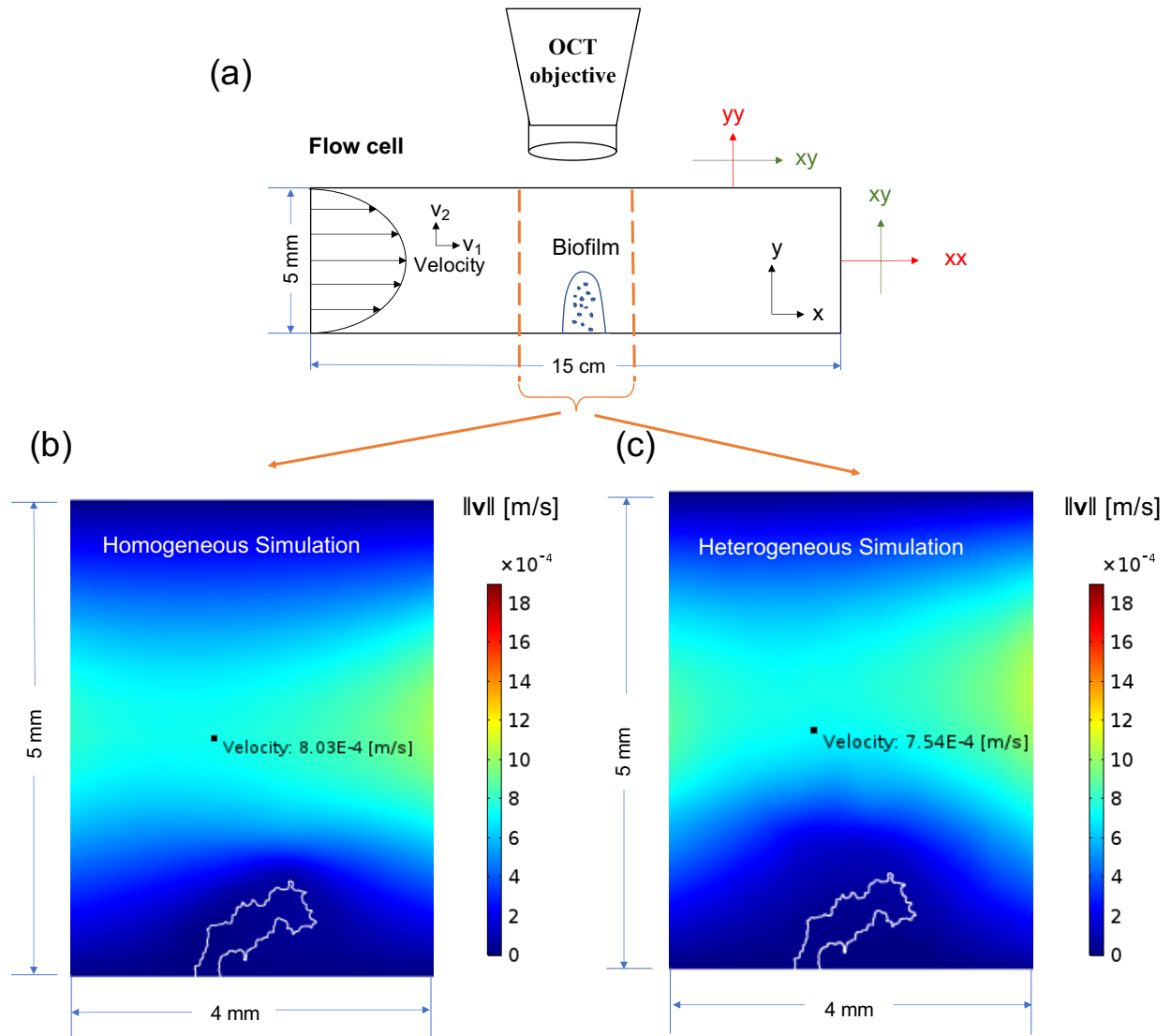


Figure 4. Schematic of experimental setup, modeling coordinate system (a) and simulated magnitude of velocity $||\mathbf{v}||$ for homogeneous biofilm (b) and heterogeneous biofilm (c) at $t=8s$.

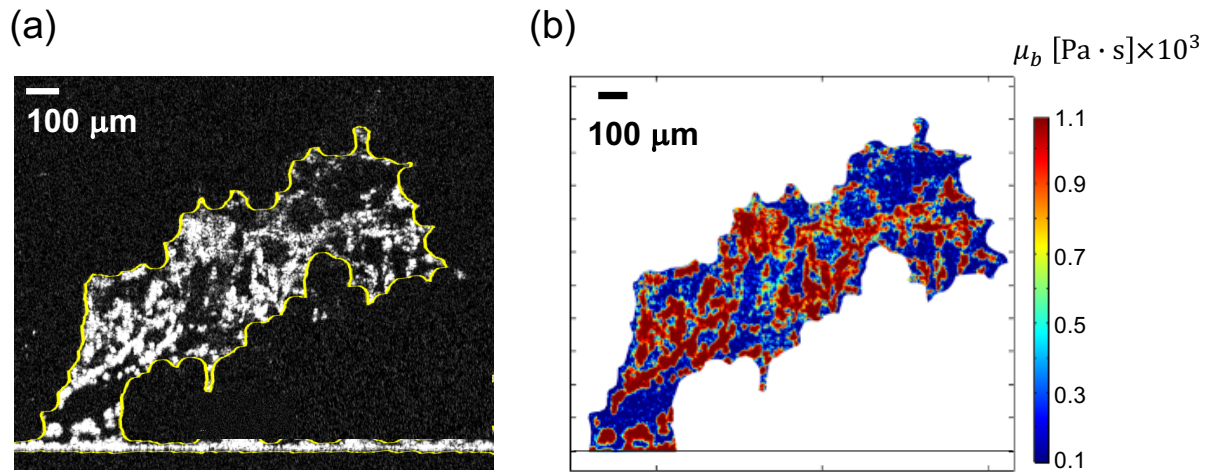
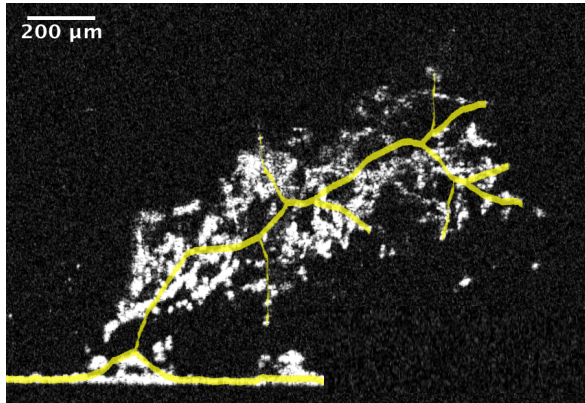


Figure 5. The map of biofilm non-Newtonian viscosity μ_b . (a) 2D OCT biofilm image with extracted boundary highlighted yellow. The unrelated data were filtered out. (b) The 2D spatial distribution of non-Newtonian viscosity that implemented in the heterogeneous biofilm simulation.

(a)



(b)

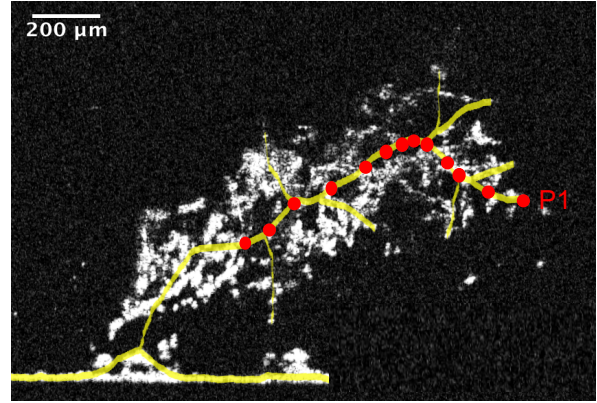


Figure 6. (a) A skeleton of stagnant biofilm (time=0). The skeleton was highlighted with a 21-pixel length yellow curve. (b) The positions of 13 tracking markers along the main skeleton of biofilms. P1 shows the first tracking point on the skeleton tip. Unrelated data were filtered out.

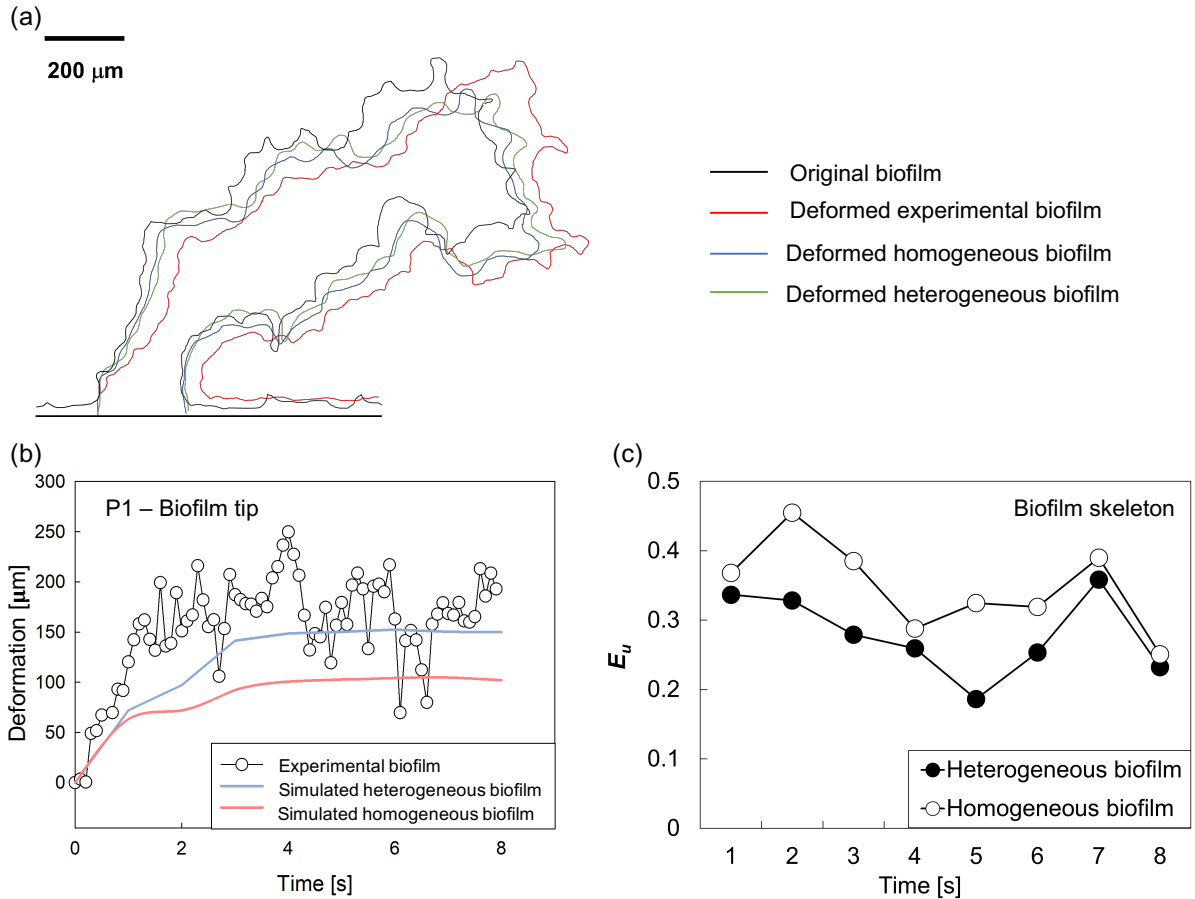


Figure 7. The comparison of biofilm boundaries and displacements of the skeleton and point P1. Flow was from left to right. (a) The comparison of biofilm boundaries. Black line: biofilm contour at $t=0$ (in experiment and computational model); red line: biofilm contour at $t=8$ s (in experiment); blue line: biofilm contour at $t=8$ s (in homogeneous simulation); green line: biofilm contour at $t=8$ s (in heterogeneous simulation). Unrelated data were filtered out. (b) The deformation of marker point P1 over time for the biofilm in experiment, homogeneous simulation, and heterogeneous simulation. (c) The relative deformation error E_u over time in the heterogeneous simulation and homogeneous simulation for all 13 marker points along the skeleton. See Figure 6 for location of skeleton points, including P1.

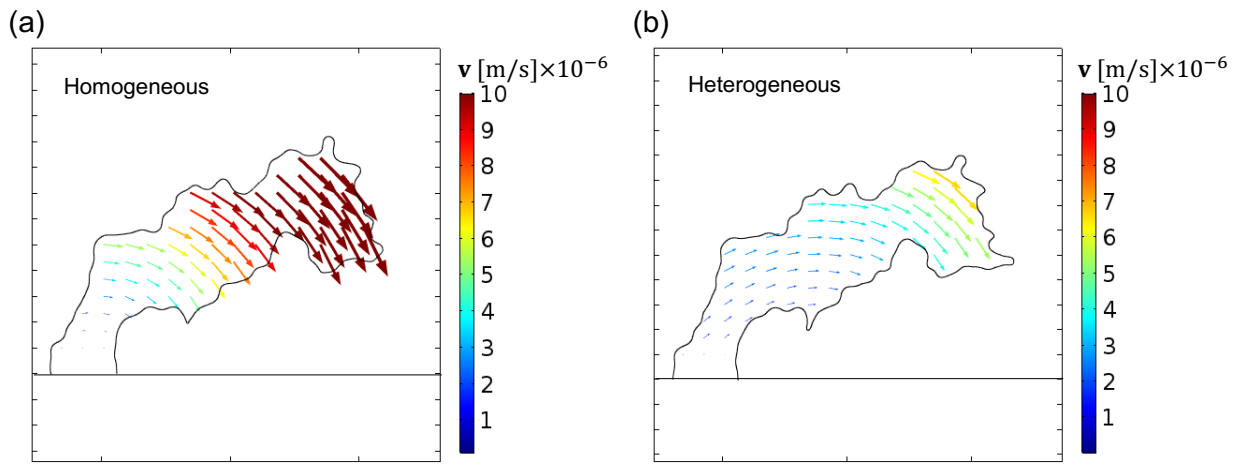


Figure 8. The simulated biofilm velocity v at $t=8$ for homogeneous simulation (a) and heterogeneous simulation (b).

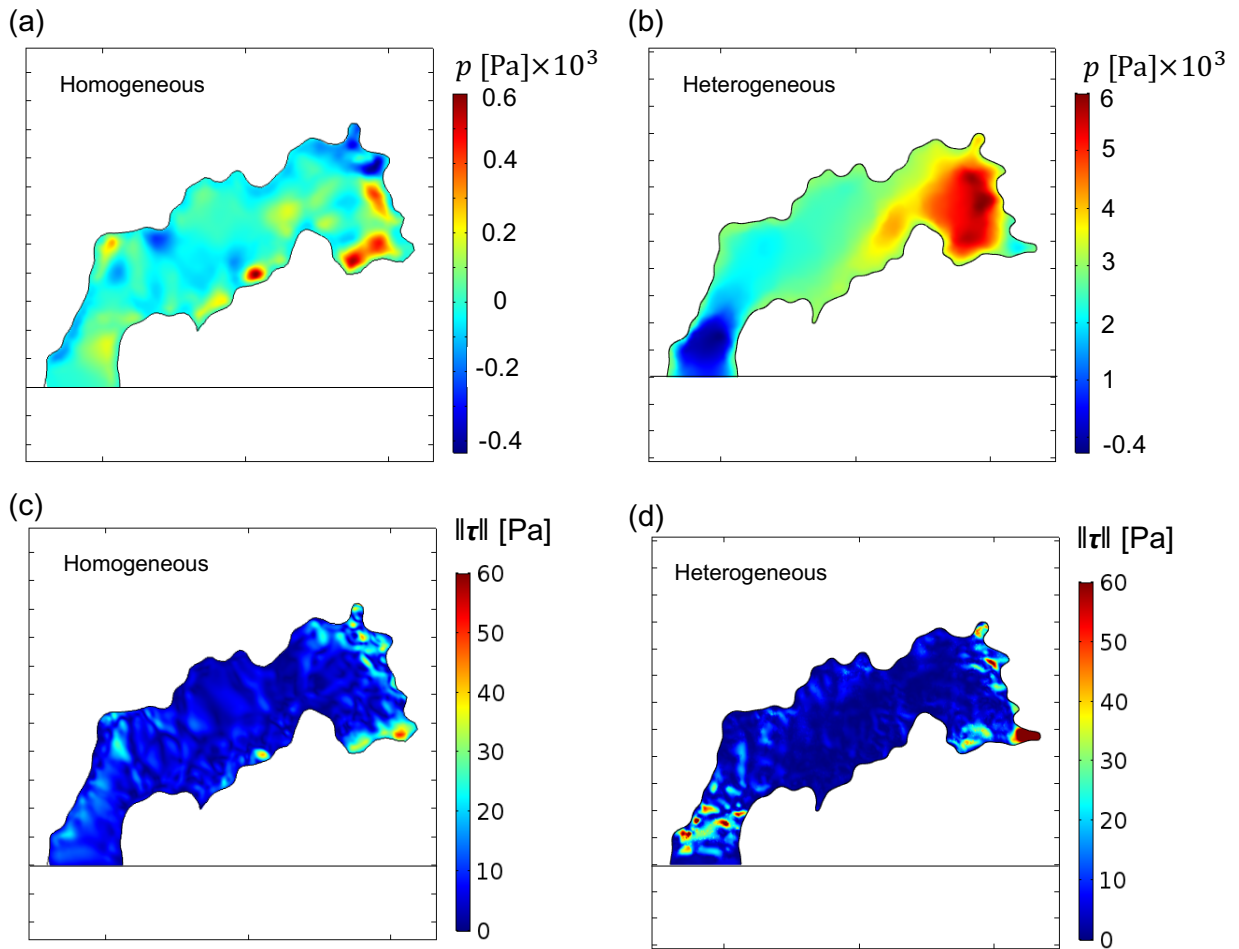


Figure 9. Simulated pressure p and magnitude of the biofilm extra stress tensor $||\tau||$ at $t=8$ for homogeneous simulation (a&c) and heterogeneous simulation (b&d).